Cancer Nano (2010) 1:71–78
DOI 10.1007/s12645-010-0009-x

ORIGINAL PAPER

Investigating the specific uptake of EGF-conjugated nanoparticles in lung cancer cells using fluorescence imaging

Honglin Jin · Jonathan F. Lovell · Juan Chen · Kenneth Ng · Weiguo Cao · Lili Ding · Zhihong Zhang · Gang Zheng

Received: 15 October 2010 / Accepted: 27 October 2010 / Published online: 11 November 2010

Abstract Targeted nanoparticles have the potential to deliver a large drug payload specifically to cancer cells. Targeting requires that a ligand on the nanoparticle surface interact with a specific membrane receptor on target cells. However, the contribution of the targeting ligand to nanoparticle delivery is often influenced by non-specific nanoparticle uptake or secondary targeting mechanisms. In this study, we investigate the epidermal growth factor (EGF) receptor-targeting specificity of a nanoparticle by dual-color fluorescent labeling. The targeted nanoparticle was a fluorescently labeled, EGF-conjugated HDL-like peptide–phospholipid scaffold (HPPS) and the cell lines expressed EGF receptor linked with green fluorescent protein (EGFR-GFP). Using LDLA7 cells partially expressing EGFR-GFP, fluorescence imaging demonstrated the co-internalization of EGFR-GFP and EGF-HPPS, thus validating its targeting specificity. Furthermore, specific EGFR-mediated uptake of the EGF-HPPS nanoparticle was confirmed using human non-small cell lung cancer A549 cells. Subsequent confocal microscopy and flow cytometry studies delineated how secondary targeting mechanisms affected the EGFR targeting. Together, this study confirms the EGFR targeting of EGF-HPPS in lung cancer cells and provides insight on the potential influence of unintended targets on the desired ligand–receptor interaction.

Keywords Nanoparticles · GFP · EGF · Lung cancer · Targeting specificity

H. Jin · J. F. Lovell · J. Chen · K. Ng · W. Cao · L. Ding · G. Zheng
Ontario Cancer Institute and Campbell Family Cancer Research Institute, University of Toronto,
Toronto, Canada

H. Jin · W. Cao · G. Zheng
Department of Medical Biophysics, University of Toronto,
Toronto, Canada

H. Jin · Z. Zhang (✉)
Britton Chance Center for Biomedical Photonics,
Wuhan National Laboratory for Optoelectronics–Huazhong University of Science and Technology,
Wuhan, China

J. F. Lovell · K. Ng · G. Zheng (✉)
Institute of Biomaterials and Biomedical Engineering,
University of Toronto,
Toronto, Canada
e-mail: gang.zheng@uhnres.utoronto.ca

Z. Zhang
e-mail: czyzzh@mail.hust.edu.cn

1 Introduction

Nanoparticle-based drug delivery is on the verge of revolutionizing cancer therapy due to superior drug solubility, improved serum stability, longer circulation half-lives, better drug loading and shielding ability, and excellent drug accumulation in tumor through the enhanced permeability and retention effect (Brigger et al. 2002; Petros and DeSimone 2010). External ligands, including antibodies, proteins, peptides, aptamers, and other small molecule ligands can be attached to nanoparticle carriers (Brannon-Peppas and Blanchette 2004; Byrne et al. 2008; Lammers et al. 2008), resulting in targeted nanoparticles. When integrating a targeting ligand with a nanoparticle, the resulting targeting efficiency may be influenced by many factors, such as the ligand numbers (Jiang et al. 2008), the ligand coupling method and site of ligand coupling (Zheng et al. 2005), the interaction between the ligand and nanoparticle (Vincent et al. 2009), as well as non-specific

binding caused by nanoparticle itself (Chen et al. 2010). Therefore, validation of targeting effects for a given ligand may be difficult to resolve with traditional competition–inhibition methods using an excess of free ligand or simple models via positive–negative cells (Yu et al. 2010). This is further complicated by the heterogeneous nature of tumor cells (Poste et al. 1982). Co-expression of different receptors or biomarkers on the cell surface may complicate the desired ligand–receptor interaction, which may lead to false-positive or negative results that obscure the understanding of how nanoparticle targeting works.

We recently reported a HDL-mimicking peptide–phospholipid scaffold (HPPS) nanocarrier for the delivery of diagnostic and therapeutic payloads (Zhang et al. 2009). HPPS closely resembles the structure of plasma-derived spherical HDL by replacing apoA-I protein with self-assembled apoA-I mimetic peptides on the phospholipid monolayer of the nanoparticle (Zhang et al. 2009). This results in nanoparticles of well-controlled, monodispersed, sub-30 nm size, that retain the HDL-like capacity to carry lipophilic payloads. Perhaps equally important, HPPS mimics the functions of plasma-derived HDL in its pharmacokinetics and targeting specificity against scavenger receptor type B1 (SR-BI), which permits excellent delivery of the nanoparticle cargo to the target cells. Furthermore, like HDL (Corbin et al. 2007), HPPS can be tailored to target a receptor of choice by introducing various targeting ligands for different cancer applications.

Epidermal growth factor receptor (EGFR), a member of the human epidermal growth factor receptor (HER)–ErbB family of receptor tyrosine kinases, represents an important target for non-small cell lung cancer diagnosis and treatment. Its activation stimulates key processes involved in tumor growth and progression, including proliferation, angiogenesis, invasion, and metastasis. Therefore, EGFR has become an attractive target for nanoparticle-based lung cancer detection and treatment (Doroshow 2005; Gatzemeier 2003). Many EGFR-specific targeting ligands (antibodies, single chain antibody fragments, affibodies, recombinant epidermal growth factor (EGF), EGF peptide mimetics, etc.) have been developed and used to target nanoparticle carriers to EGFR (Dechant et al. 2007; Nakamura et al. 2005; Reilly et al. 2000; Senekowitsch-Schmidtke et al. 1996; Tolmachev et al. 2009) with various degrees of success. Targeting nanoparticles to EGFR in lung cancer provides a desirable model to study the complexities of ligand/nanoparticle–receptor interactions. Previously, we have successfully developed an EGF-conjugated HPPS nanoparticle and tested its targeting to cancer cells in vitro and in vivo (Zhang et al. 2010). The objective of this study is to take advantage of this already established targeted nanoparticle model to systematically investigate the receptor specific uptake of EGF-conjugated nanoparticles in lung cancer cells, thus providing valuable insight on the potential impact of tumor cell heterogeneity on the targeting specificity of nanoparticle carriers.

2 Materials and methods

2.1 Preparation of EGF-conjugated HPPS nanoparticle

Human EGF was obtained from R&D Systems, Inc. (USA). EGF-HPPS was generated as previously described (Zhang et al. 2010). In brief, EGF was treated with Traut's reagent to make sulfhydryl-activated EGF. HPPS containing DSPE-PEG (2000) maleimide and loaded with the near-infrared fluorescent dye DiR-BOA was then mixed with sulfhydryl-activated EGF at room temperature for 20 h. The EGF-conjugated HPPS particle, termed EGF-HPPS, was subsequently filtered (0.2 μm) and purified by gel filtration chromatography using the Akta FPLC system (Amersham Biosciences, USA) equipped with a HiLoad 16/60 Superdex 200 pg column.

2.2 Cell culture

Cell culture media RPMI 1640 and Hams F-12, along with fetal bovine serum (FBS) and Geneticin (G418) were purchased from Gibco-Invitrogen Co. (USA). LdlA7 cells, which minimally express EGFR and scavenger receptor class B type I ($EGFR^-$, $SR\text{-}BI^-$), were kindly provided by Dr. Monty Krieger (Massachusetts Institute of Technology, Cambridge, MA). LdlA7 cells were cultured in Hams F-12 media with 2 mM L-glutamine, 100 U/ml penicillin–streptomycin, and 5% FBS. Human lung adenocarcinoma A549 cell line ($EGFR^+$, $SR\text{-}BI^+$) and human lung squamous cell carcinoma NCL-H520 cell line ($SR\text{-}BI^+$, $EGFR^-$) were purchased from the American Type Culture Collection. A549 cells and H520 cells were cultured in RPMI-1640 medium supplemented with 10% FBS. All cells were grown at 37°C in a humidified atmosphere containing 5% CO_2.

2.3 Plasmid transfection

Plasmid transfections of pCDNA-EGFR-EGFP (provided by Dr. Peter Verveer, Ludwig Institute for Cancer Research, Royal Melbourne Hospital, Australia) were performed on LDLA7 and A549 cells using Lipofectamine 2000 (Invitrogen) according to the manufacturer' protocol. Transfected cells were then exposure to Geneticin (800 μg/ml) and sorted by the flow cytometry equipped with a Becton Dickinson FACS Aria cell sorter to select the cells with EGFR-GFP expressing.

2.4 Confocal microscopy and flow cytometry

Cells were seeded into 8-well cover glass-bottom chambers (Nunc Lab-Tek, Sigma-Aldrich, 2×10^4/well) for the confocal microscopy imaging and into 6-well cell culture plates (3×10^5/well) for the flow cytometry study. AF555-EGF (Alexa Fluor® 555 EGF complex, Molecular Probes, Inc., USA) was used as a standard probe to identify the EGFR positive cells. Final concentration (2.5 μg/ml) of AF555-EGF was used in confocal imaging and flow cytometry analysis. To evaluate the uptake specificity of HPPS particles, cells were incubated with HPPS or EGF-HPPS with DiR-BOA concentration at 1 μM in cell culture medium containing 10% FBS for 3 h at 37°C. The total volume of incubation medium was 300 μl/well for confocal imaging and 1 ml/well for flow cytometry. For the competition assay, cells were coincubated with an 800-M excess of HDL (1 mg/ml) or 5.6 μM EGF. Confocal imaging was taken by Olympus FV1000 laser confocal scanning microscopy (Olympus, Tokyo, Japan) with the excitation wavelength of 488 (GFP), 543 (AF555), and 633 nm (DiR-BOA). For the flow cytometry study, the fluorescence signal of cells were detected by a Dako Cytomation MoFlo 9-color cell sorter for AF555 (ex. 543 nm) and a Beckman Coulter FC500 5-color analyzer for GFP (ex. 488 nm) and DiR-BOA (ex. 633 nm).

3 Results and discussion

3.1 Establishing the correlation between EGFR expression in cells and EGF uptake using fluorescence imaging

To understand the EGFR specificity of EGF-HPPS nanoparticles, two cell lines were chosen based on their endogenous expression of EGFR (the receptor specific for the EGF ligand) and SR-BI (the receptor with affinity for the HPPS nanoparticle). Immunoblotting analysis showed that LDLA7 cells expressed low levels of both EGFR and SR-B1 ($EGFR^-$, $SR\text{-}BI^-$) whereas A549 cells expressed high levels of EGFR and moderate levels of SR-B1 ($EGFR^+$, $SR\text{-}BI^+$; data not shown). To quantify the correlation between EGF uptake and EGFR expression level, a fluorescent surrogate of EGF, AF555-EGF (biotinylated EGF conjugated with an Alexa Fluor 555-streptavidin) was used to enable sensitive detection of EGFR. Meanwhile, we transfected both LDLA7 and A549 cells with a plasmid encoding an EGFR-GFP. The EGFR-GFP-LDLA7 cells were established with only partial EGFR-GFP expression on LDLA7 cells with no endogenous EGFR expression. This is a useful model as the fluorescence of the EGFR-GFP served as a convenient measure of EGFR expression and the partial transfection created internal EGFR positive and negative controls. Once the EGFR-GFP-LDLA7 cell line was established, it was characterized using AF555-EGF together with real-time confocal microscopy. Upon incubation with AF555-EGF, confocal fluorescence imaging revealed the EGFR-mediated, time-dependent formation of endocytotic vesicles and their subsequent internalization (Fig. 1a). The highly co-localized fluorescent signals from AF555 and GFP also confirmed the intact EGFR function of EGFR-GFP expressed on the LDLA7 cell surface (Fig. 1a). As shown in Fig. 1b, cells that had high expression levels of EGFR-GFP took up the most AF555-EGF. A strong positive linear correlation (R^2=0.98) was found between the expression level of EGFR-GFP and the uptake of AF555-EGF (Fig. 1c). Thus, the correlation between the differential receptor expression levels in the partially transfected LDLA7 cells and the ligand uptake pattern in those same cells are useful to confirm EGFR-specific uptake. We next examined the A549 lung cancer cells expressing EGFR-GFP. The stably expressing EGFR-GFP-A549 cell line was established through cell sorting where higher expression of EGFR than native A549 cells was induced with EGFR-GFP. As expected, AF555-EGF was internalized with strong co-localization with the EGFR-GFP (Fig. 2a). Correlation between EGFR-GFP expression levels and AF555-EGF uptake in A549 cells was also observed using dual channel analysis using flow cytometry (Fig. 2b). The co-localization of AF555 and GFP signals clearly indicated the internalization of AF555-EGF through EGFR-mediated endocytosis pathway. Thus, two cell lines, EGFR-GFP-LDLA7 and EGFR-GFP-A549, were successfully constructed and validated for specific EGF uptake. These cell models provide a solid framework to further analyze and validate nanoparticle targeting of EGFR expressing cells.

3.2 Evaluating the specific uptake of EGF-HPPS using EGFR-GFP-LDLA7 and EGFR-GFP-A549 cells

A schematic depiction of EGF-HPPS is shown in Fig. 3a. EGF was conjugated to the surface of HPPS and the fluorescent cargo DiR-BOA was loaded into the core of HPPS. Three-dimensional and dual-color confocal imaging was used to evaluate the EGFR-mediated nanoparticle endocytosis. Upon incubation with EGFR-GFP-A549 cells, DiR-BOA from EGF-HPPS co-localized with the GFP signal in EGFR-GFP-A549 cells (Fig. 3b). This confirmed the uptake and co-localization of EGF-HPPS by EGFR. We next used EGFR-GFP-LDLA7 cells to evaluate the target specificity of EGF-HPPS (Fig. 4). When incubated with the unconjugated HPPS nanoparticle, cells had no DiR-BOA uptake. In contrast, incubation EGF-HPPS with EGFR-GFP-LDLA7 cells revealed significant DiR-BOA uptake

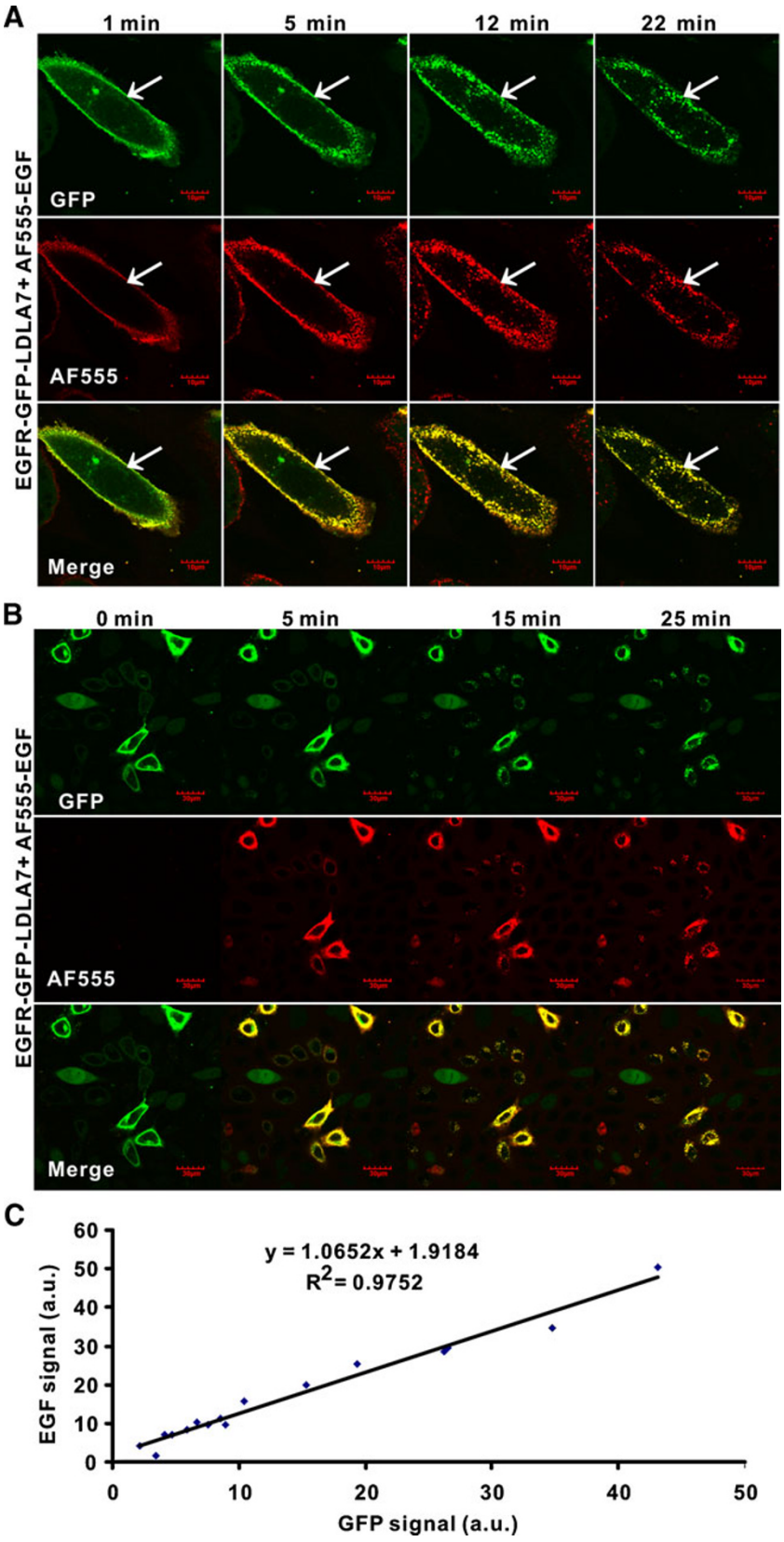

Fig. 1 A partial transfection assay reveals EGRF-GFP and EGF uptake and co-localization. **a** Real-time visualization of co-internalization of AF555-EGF and EGFR-GFP by EGFR-GFP-LDLA7 cells. **b** Visualization of cellular uptake of AF555-EGF by EGFR-GFP-A549 cells. **c** Analysis of GFP expression versus AF555-EGF uptake from confocal images. Data was acquired from 16 cells

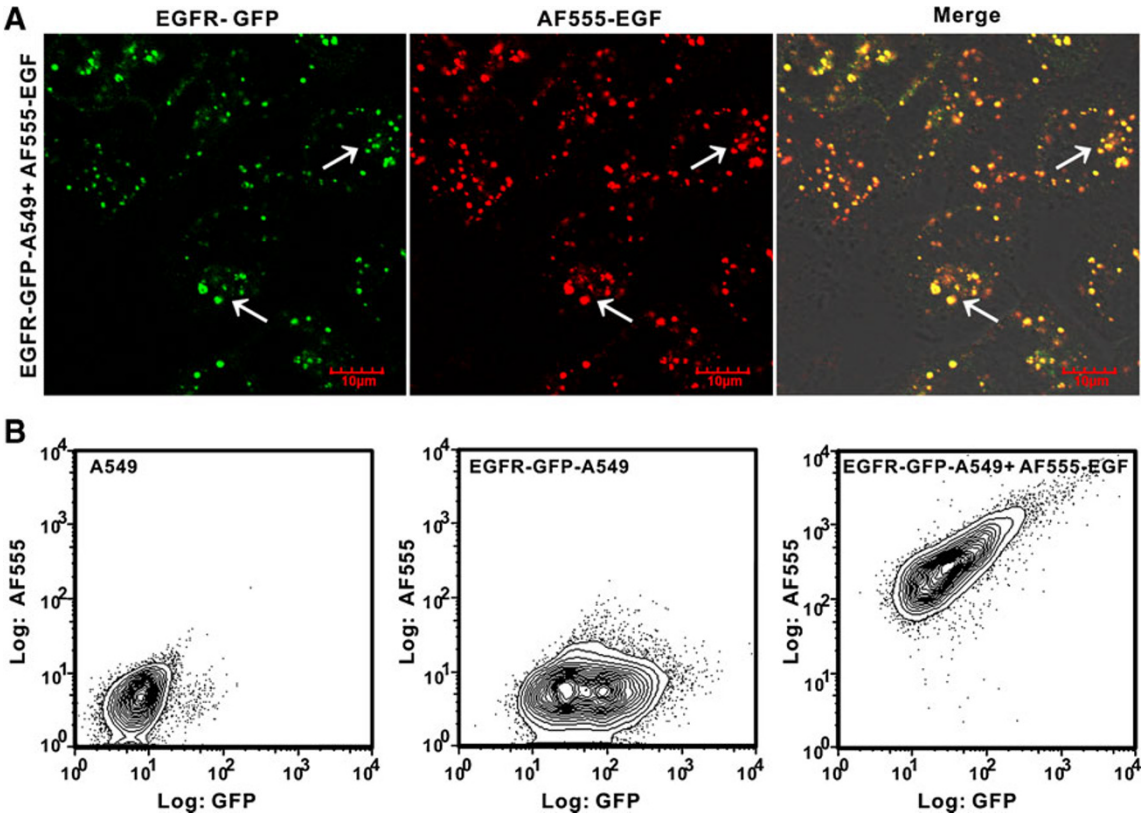

Fig. 2 EGF uptake in lung cancer cell lines. **a** Confocal images of cellular uptake of AF555-EGF by EGFR-GFP-A549 cells. **b** Quantification of GFP expression versus AF555-EGF uptake by flow cytometry. As shown from *left* to *right*, A549 cells alone (*left*), EGFR-GFP-A549 cells alone (*middle*), and EGFR-GFP-A549 cells treated with AF555-EGF (*right*), respectively

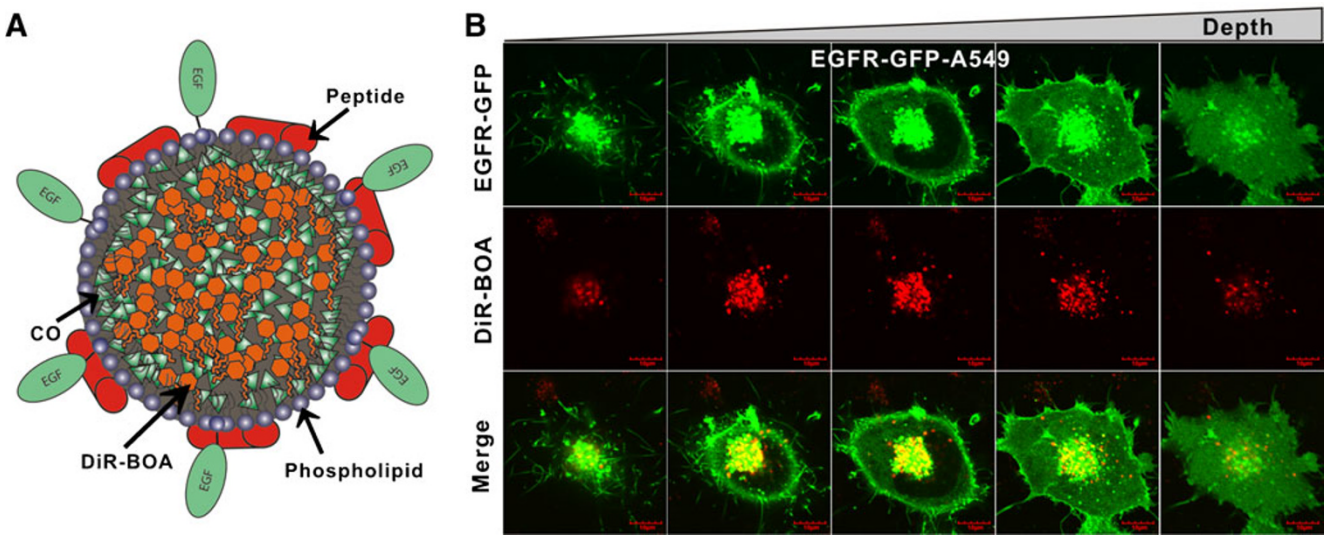

Fig. 3 EGF targeting of payload bearing nanoparticles. **a** Schematic figure of EGF-HPPS. EGF-HPPS consists of phospholipids, peptides, cholesteryl oleate (CO), DiR-BOA cargo, and EGF. **b** Three-dimensional imaging of uptake of EGF(DiR-BOA) HPPS by EGFR-GFP-A549 cells

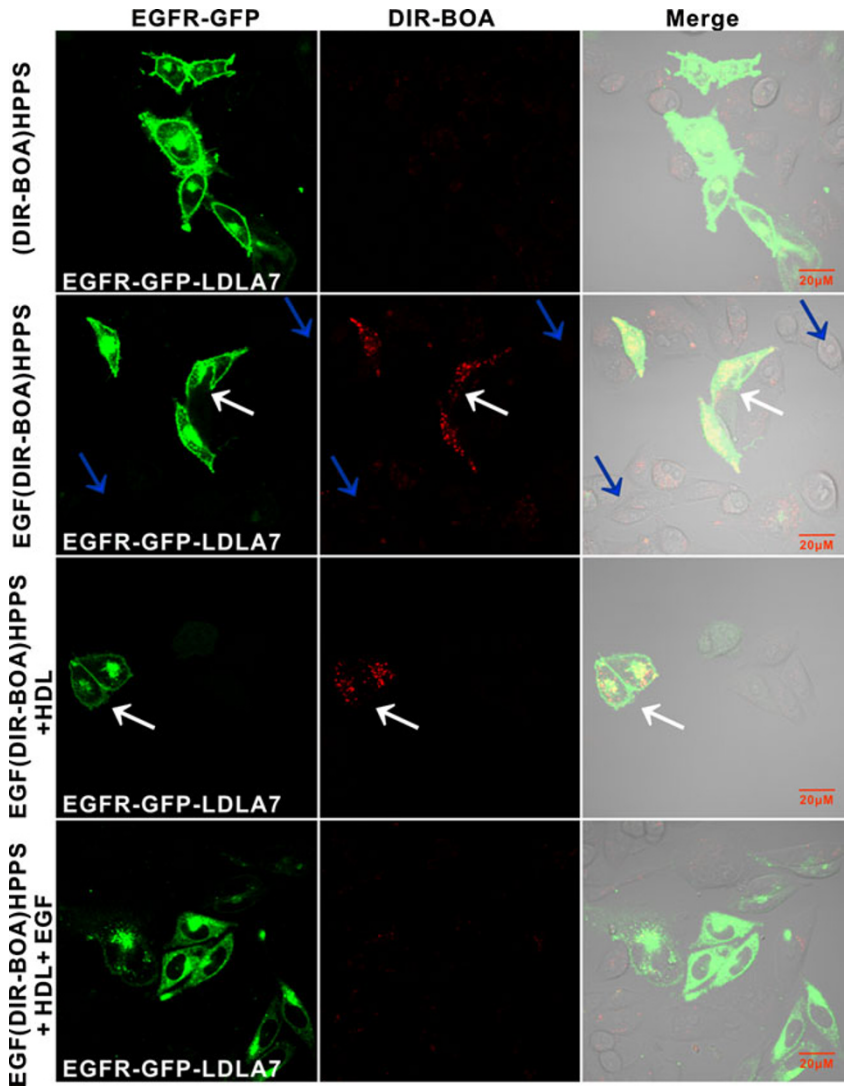

Fig. 4 A partial transfection assay validates EGFR-directed nanoparticle uptake of EGF-HPPS. Cellular uptake of (DiR-BOA)HPPS, EGF (DiR-BOA)HPPS, EGF(DiR-BOA)HPPS with HDL or EGF(DiR-BOA)HPPS with excess of HDL, and EGF by EGFR-GFP-LDLA7 cells. *White arrow* represents specific uptake of EGF(DiR-BOA)HPPS through EGFR-mediated pathway. *Blue arrow* indicates the cells without EGFR-GFP expression have no uptake of EGF(DiR-BOA)HPPS

(white arrow). Importantly, cells without any EGFR-GFP expression (internal EGFR negative control) did not display any detectable DiR-BOA uptake (blue arrows). This demonstrates that EGF-HPPS specifically delivered its cargo (DiR-BOA) to target cells via EGFR-mediated endocytosis. To rule out the potential interference of native HDL on the EGF-HPPS targeting, the same cells were incubated with EGF-HPPS, along with excess HDL and/or EGF. Confocal images illustrated that there was no change to the specific uptake of EGF-HPPS in the presence of HDL alone. However, the specific uptake of EGF-HPPS was inhibited by addition of excess EGF. These data confirmed the EGFR-targeting ability of EGF-HPPS.

In a more complex scenario, H520 cells ($EGFR^{-}$, $SR\text{-}B1^{+}$), A549 cells ($EGFR^{+}$, $SR\text{-}B1^{+}$), and EGFR-GFP-A549 ($EGFR^{++}$, $SR\text{-}B1^{+}$), with various EGFR expression levels from negative, positive to strongly positive, were used to quantify the specific uptake of EGF-HPPS. It should be noted that both A549 and H520 cells are positive for SR-B1 receptor ($SR\text{-}B1^{+}$), which has natural affinity for HDL (Acton et al., 1996) and for apoA-1 mimetic helical peptides (Wool et al., 2008; Zhang et al., 2010). Therefore, the secondary targeting of SR-BI along with the targeting to EGFR was investigated using confocal microscopy and flow cytometry. First, EGFR-GFP-A549 cells were incubated with EGF-HPPS alone, with excess HDL or with excess of both HDL and EGF. As shown in Fig. 5a, the uptake of EGF-HPPS by EGFR-GFP-A549 cells was completely inhibited when both excess HDL and EGF were added but not with only HDL, which is indicative of EGFR targeting. Under the same condition when using H520 cells ($EGFR^{-}$, $SR\text{-}BI^{+}$), very weak fluorescent signal was detected for EGF-HPPS presumably due to the SR-BI pathway (Fig. 5b). This secondary targeting was further confirmed by the diminished signal in the presence of excess HDL (Fig. 5b). Further

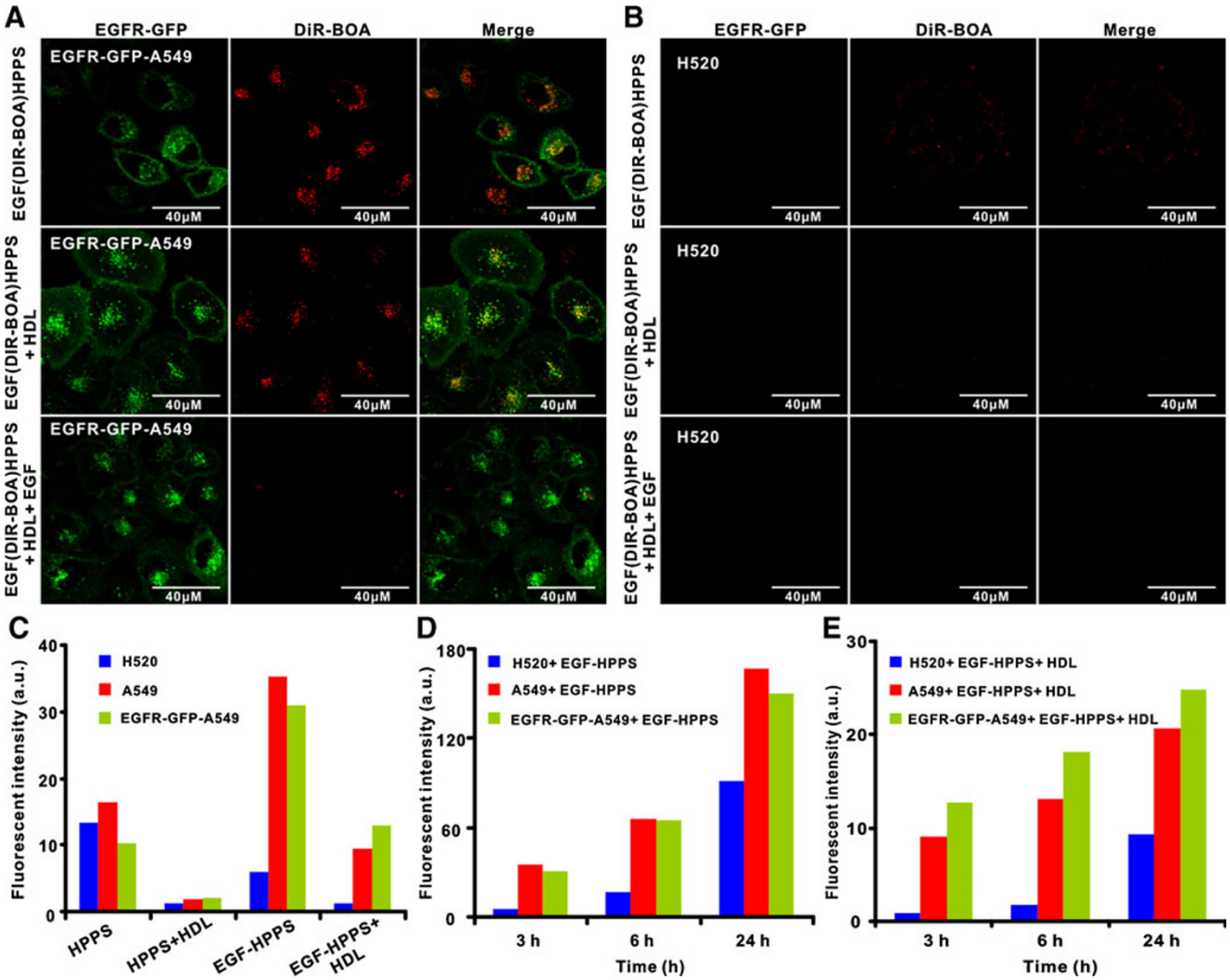

Fig. 5 EGF-HPPS as nanoprobe for targeting lung cancer cells expressing high level of EGFR in vitro. Confocal imaging of distinguished uptake of EGF-HPPS between: **a** EGFR positive A549 cells and **b** EGFR negative H520 cells. **c** Quantification of cellular uptake of HPPS, HPPS with excess of HDL, EGF-HPPS, EGF-HPPS with excess of HDL or EGF-HPPS with excess of HDL and EGF by H520, A549, and EGFR-GFP-A549 cells within 3 h incubation. **d** Quantification of cellular uptake of EGF-HPPS by H520, A549, and EGFR-GFP-A549 cells during 3, 6, and 24 h incubation by flow cytometry. **e** Quantification of cellular uptake of EGF-HPPS by H520, A549, and EGFR-GFP-A549 cells with excess of HDL

evidence on the influence of secondary targeting was obtained using flow cytometry. As shown in Fig. 5c, HPPS (in the absence of EGF ligand) was taken up via SR-BI pathway in H520, A549, and EGFR-GFP-A549 cells (Fig. 5c, 1st column), but their uptake were all inhibited by excess of HDL (Fig. 5c, 2nd column). The 6.3-fold difference in the uptake of EGF-HPPS between A549 cells and H520 cells (Fig. 5c, 3rd column) was probably due to differential EGFR expression levels and the shielding of SR-BI recognition by EGF conjugation, evidenced by a 2.2-fold increase in EGF-HPPS uptake by A549 cells but a 2.3-fold decrease by H520 cells (Fig. 5c, 3rd versus 1st column). Furthermore, HDL blocking enhanced the EGF-HPPS uptake contrast between A549 cells and H520 cells from 6.3-fold (Fig. 5c, 3rd column) to 9.7-fold (Fig. 5c, 4th column). Next, uptake of EGF-HPPS by H520, A549, and EGFR-GFP-A549 cells with or without excess of HDL were evaluated at 3, 6, and 24 h after incubation (Fig. 5d and e). At all three time points, the difference of EGF-HPPS uptake between A549 ($EGFR^{+}$) and EGFR-GFP-A549 ($EGFR^{++}$) could not be distinguished without the excess of HDL which blocks secondary SR-BI targeting (Fig. 5d). Clear differences only appeared after adding excess of HDL, which revealed the pure EGFR targeting (Fig. 5e). Another interesting effect of this secondary targeting lies in the fact both EGFR and SR-BI contributed to the EGF-HPPS uptake. This observation could be explored for enhancing the uptake through dual receptor coordination.

We have validated the specific uptake of EGF-HPPS nanoparticles via the EGFR pathway as well as the secondary targeting via SR-BI pathway using dual fluorescent labeling approach (labeling both the nanoparticles and cell lines). The use of double negative LDLA7 cells ($EGFR^-$ and $SR\text{-}BI^-$) established a clear baseline for EGFR-GFP partial transfection to create internal $EGFR^+$ and $EGFR^-$ controls. On the other hand, the use of both EGFR-GFP-A549 cells ($EGFR^{++}$) and wild-type A549 cells ($EGFR^+$) together with the use of H520 cells ($EGFR^-$) allowed us to analyze the EGF/EGFR response at different levels of EGFR expression in lung cancer cells.

In summary, this study confirmed the EGFR targeting of EGF-HPPS in lung cancer cells. More importantly, the dual fluorescent labeling approach (labeling both the ligand-conjugated nanoparticle carrier and the targeted receptors on the cells) developed in this study provides more insight on the potential influence of secondary targets on the intended ligand–receptor interaction. Furthermore, this fluorescent imaging strategy may be applied for target validation in other applications such as confirming the putative target receptor for a ligand of interest.

Acknowledgments This study was conducted with the support of the Ontario Institute for Cancer Research through the Government of Ontario, the Canadian Institute of Health Research, the Natural Sciences and Engineering Research Council of Canada, the China-Canada Joint Health Research Initiative (CIHR CCI-102936, NSFC-30911120489), the Ontario Ministry of Health and Long Term Care, and the Joey and Toby Tanenbaum/Brazilian Ball Chair in Prostate Cancer Research.

References

Acton S, Rigotti A, Landschulz KT, Xu S, Hobbs HH, Krieger M (1996) Identification of scavenger receptor SR-BI as a high density lipoprotein receptor. Sci NY NY 271(5248):518–520

Brannon-Peppas L, Blanchette JO (2004) Nanoparticle and targeted systems for cancer therapy. Adv Drug Deliv Rev 56(11):1649–1659

Brigger I, Dubernet C, Couvreur P (2002) Nanoparticles in cancer therapy and diagnosis. Adv Drug Deliv Rev 54(5):631–651

Byrne JD, Betancourt T, Brannon-Peppas L (2008) Active targeting schemes for nanoparticle systems in cancer therapeutics. Adv Drug Deliv Rev 60(15):1615–1626

Chen H, Wang L, Yeh J, Wu X, Cao Z, Wang YA, Zhang M, Yang L, Mao H (2010) Reducing non-specific binding and uptake of nanoparticles and improving cell targeting with an antifouling PEO-b-PgammaMPS copolymer coating. Biomaterials 31(20):5397–5407

Corbin I, Chen J, Cao W, Lin H, Lund-Katz S, Zheng G (2007) Enhanced cancer-targeted delivery using engineered high-density lipoprotein-based nanocarriers. J Biomed Nanotechnol 3(4):367–376

Dechant M, Beyer T, Schneider-Merck T, Weisner W, Peipp M, van de Winkel JG, Valerius T (2007) Effector mechanisms of recombinant IgA antibodies against epidermal growth factor receptor. J Immunol 179(5):2936–2943

Doroshow JH (2005) Targeting EGFR in non-small-cell lung cancer. N Engl J Med 353(2):200–202

Gatzemeier U (2003) Targeting the HER1/EGFR receptor to improve outcomes in non-small-cell lung cancer. Oncol Williston Park NY 17(11 Suppl 12):7–10

Jiang W, Kim BY, Rutka JT, Chan WC (2008) Nanoparticle-mediated cellular response is size-dependent. Nat Nanotechnol 3(3):145–150

Lammers T, Hennink WE, Storm G (2008) Tumour-targeted nanomedicines: principles and practice. Br J Cancer 99(3):392–397

Nakamura T, Takasugi H, Aizawa T, Yoshida M, Mizuguchi M, Mori Y, Shinoda H, Hayakawa Y, Kawano K (2005) Peptide mimics of epidermal growth factor (EGF) with antagonistic activity. J Biotechnol 116(3):211–219

Petros RA, DeSimone JM (2010) Strategies in the design of nanoparticles for therapeutic applications. Nat Reviews 9(8):615–627

Poste G, Tzeng J, Doll J, Greig R, Rieman D, Zeidman I (1982) Evolution of tumor cell heterogeneity during progressive growth of individual lung metastases. Proc Natl Acad Sci USA 79 (21):6574–6578

Reilly RM, Kiarash R, Sandhu J, Lee YW, Cameron RG, Hendler A, Vallis K, Gariepy J (2000) A comparison of EGF and MAb 528 labeled with 111In for imaging human breast cancer. J Nucl Med 41(5):903–911

Senekowitsch-Schmidtke R, Steiner K, Haunschild J, Mollenstadt S, Truckenbrodt R (1996) In vivo evaluation of epidermal growth factor (EGF) receptor density on human tumor xenografts using radiolabeled EGF and anti-(EGF receptor) mAb 425. Cancer Immunol Immunother 42(2):108–114

Tolmachev V, Friedman M, Sandstrom M, Eriksson TL, Rosik D, Hodik M, Stahl S, Frejd FY, Orlova A (2009) Affibody molecules for epidermal growth factor receptor targeting in vivo: aspects of dimerization and labeling chemistry. J Nucl Med 50(2):274–283

Vincent A, Babu S, Heckert E, Dowding J, Hirst SM, Inerbaev TM, Self WT, Reilly CM, Masunov AE, Rahman TS, Seal S (2009) Protonated nanoparticle surface governing ligand tethering and cellular targeting. ACS Nano 3(5):1203–1211

Wool GD, Reardon CA, Getz GS (2008) Apolipoprotein A-I mimetic peptide helix number and helix linker influence potentially anti-atherogenic properties. J Lipid Res 49(6):1268–1283

Yu DH, Lu Q, Xie J, Fang C, Chen HZ (2010) Peptide-conjugated biodegradable nanoparticles as a carrier to target paclitaxel to tumor neovasculature. Biomaterials 31(8):2278–2292

Zhang Z, Cao W, Jin H, Lovell JF, Yang M, Ding L, Chen J, Corbin I, Luo Q, Zheng G (2009) Angew Chem Int 48(48):9171–9175

Zhang Z, Chen J, Ding L, Jin H, Lovell JF, Corbin IR, Cao W, Lo PC, Yang M, Tsao MS, Luo Q, Zheng G (2010) HDL-mimicking peptide-lipid nanoparticles with improved tumor targeting. Small Weinheim Bergstrasse Ger 6(3):430–437

Zheng G, Chen J, Li H, Glickson JD (2005) Rerouting lipoprotein nanoparticles to selected alternate receptors for the targeted delivery of cancer diagnostic and therapeutic agents. Proc Natl Acad Sci USA 102(49):17757–17762